The Journal of Neuroscience, August 1990, 10(8): 2587–2600

Localization of Dopamine D_2 Receptor mRNA and D_1 and D_2 Receptor Binding in the Rat Brain and Pituitary: An *in situ* Hybridization-Receptor Autoradiographic Analysis

Alfred Mansour,[1] James H. Meador-Woodruff,[1] James R. Bunzow,[2] Olivier Civelli,[2] Huda Akil,[1] and Stanley J. Watson[1]

[1]Mental Health Research Institute, University of Michigan, Ann Arbor, Michigan 48109-0720, and [2]Vollum Institute for Advanced Biomedical Research, The Oregon Health Sciences University, Portland, Oregon 97201

Several lines of evidence suggest the existence of multiple dopamine receptor subtypes, referred to as D_1 and D_2. The present study examines the distribution of these dopamine binding sites in the rat brain and pituitary in relation to the distribution of D_2 receptor mRNA using a combination of *in vitro* receptor autoradiographic and *in situ* hybridization techniques. ^{3}H-Raclopride and ^{3}H-SCH23390 (in the presence of 1 μM ketanserin) were used to label D_2 and D_1 receptor binding sites, respectively, while a 495 bp cRNA probe synthesized from the *Sac I-Bgl II* fragment of a rat D_2 receptor cDNA was used to visualize the D_2 receptor mRNA. Analysis of adjacent tissue sections in which receptor autoradiography and *in situ* hybridization had been performed revealed several brain regions where the D_2 binding site and corresponding mRNA appear to be similarly distributed, including the caudate-putamen, nucleus accumbens, olfactory tubercle, globus pallidus, substantia nigra, and ventral tegmental area. In the pituitary gland, D_2 binding sites and mRNA appear to be codistributed with very dense levels in the intermediate lobe and individually labeled cells in the anterior lobe. Brain regions demonstrating a lack of correspondence between the distribution of the D_2 binding site and D_2 receptor mRNA include the olfactory bulb, neocortex, paleocortex, hippocampus, and zona incerta. Several hypotheses are discussed to explain the lack of correspondence in certain brain regions; these include the localization of receptor binding sites on both fibers and cell bodies and receptor transport. These studies provide a better understanding of the anatomical distribution of the D_2 receptor and serve as a framework for future regulatory and anatomical mapping studies. By focusing on specific brain regions, such as the nigrostriatal system, hippocampus, and olfactory bulb, they provide insights into D_2 receptor synthesis, transport, and insertion into cell membranes.

Received Nov. 6, 1989; revised Mar. 14, 1990; accepted Mar. 15, 1990.

We are grateful to Elizabeth Cox for her expert secretarial assistance and for grants from the National Institute for Mental Health (MH42251, MH15794, MH45614), National Alliance for the Mentally Ill, Lucille P. Markey Charitable Trust, Theophile Raphael, National Alliance for Research on Schizophrenia and Depression, and Eli Lilly (APA/Lilly Psychiatric Fellowship).

Correspondence should be addressed to Alfred Mansour, Ph.D., Mental Health Research Institute, University of Michigan, 205 Washtenaw Place, Ann Arbor, MI 48109-0720.

Cumulative evidence suggests the existence of at least 2 distinct dopaminergic receptor subtypes, referred to as D_1 and D_2. D_1 dopamine (DA) receptors are positively coupled to adenylate cyclase (Stoof and Kebabian, 1984), widely distributed in the CNS (Boyson et al., 1986; Dawson et al., 1986; Dubois et al., 1986; Bouthenet et al., 1987; Wamsley et al., 1989), and abundant in the parathyroid gland (Attie et al., 1980). D_2 DA receptors, on the other hand, are either not coupled to adenylate cyclase (Memo et al., 1986) or negatively coupled (Onali et al., 1985) and are densely distributed in the basal ganglia (Martres et al., 1985; Charuchinda et al., 1987; Joyce and Marshall, 1987; Richfield et al., 1987) and pituitary gland (Kohler and Fahlberg, 1985; Pazos et al., 1985; DeSouza, 1986).

Selective lesion studies (Creese et al., 1977; Nagy et al., 1978; Schwarcz et al., 1978; Cross and Waddington, 1981; Joyce and Marshall, 1987; Trugman and Wooten, 1987; Filloux et al., 1988; Porceddu et al., 1986) suggest that while D_1 and D_2 receptors are both localized on pre- and postsynaptic membranes, the D_2 subtype may function as an "autoreceptor," modulating the synthesis and/or release of DA. Support for this hypothesis has come from findings demonstrating that D_2 receptors can be localized on DA-containing cells (Reisine et al., 1979) and that application of selective D_2 agonists produces a decrease in cell firing (White and Wang, 1983), DA release, and synthesis (Stoof et al., 1982; Brown et al., 1985). Similar changes in DA release and turnover have not been observed with selective D_1 receptor agonists (Stoof et al., 1982; Brown et al., 1985; Clark and Galloway, 1985).

The rat D_2 receptor has been recently cloned (Bunzow et al., 1988) and is structurally similar to members of the family of G protein-coupled receptors that include the α- and β-adrenergic receptors, the muscarinic receptors and rhodopsin. Northern blot analysis suggests that the mRNA coding for the D_2 receptor shows a similar distribution to the D_2 sites reported with ligand binding, with high levels observed in the striatum and pituitary. Further, transfection of the D_2 receptor DNA into cells normally not demonstrating DA receptors results in the expression of specific D_2 receptor binding.

Given these findings, we have recently examined the distribution of the D_2 receptor mRNA using *in situ* hybridization (Meador-Woodruff et al., 1989). D_2 receptor mRNA was visualized in DA projections fields, such as the caudate-putamen, nucleus accumbens, and olfactory tubercle, as well as in dopamine-containing cell groups such as the substantia nigra (SN), ventral tegmental area (VTA), and zona incerta. Such a distri-

bution would suggest that the D_2 receptor has both a pre- and postsynaptic localization and the receptors visualized in the SN and VTA may serve as autoreceptors. Consistent with this hypothesis, unilateral 6-hydroxydopamine lesions of the DA neurons in the medial forebrain bundle produce a complete ipsilateral loss of D_2 receptor mRNA in the SN and VTA and a compensatory increase in the D_2 receptor mRNA of the denervated striatum (Mansour et al., 1990).

The purpose of the present set of studies is to compare the distribution of D_2 receptor mRNA in the brain and pituitary to D_1 and D_2 binding sites using a combination of *in situ* hybridization and *in vitro* receptor autoradiographic techniques. These anatomical studies provide a more precise analysis of the distribution of D_2 receptor mRNA and dopaminergic ligand binding sites than is possible with Northern analysis and homogenate binding. Moreover, while the transfection studies (Bunzow et al., 1988) discussed previously are essential for identifying a D_2 receptor, studies combining *in situ* hybridization and receptor autoradiography are necessary in supporting, validating, and extending these findings to the CNS.

Several quantitative studies are available describing the distribution of D_1 and D_2 binding sites in the brain (e.g., Bouthenet et al., 1987; Charuchinda et al., 1987; Wamsley et al., 1989). It is not the focus of the present study to replicate these findings, but to examine in serial sections the distribution of the mRNA encoding for the D_2 receptor in relation to the DA binding sites to gain insights into regions of possible receptor synthesis, transport, and eventual insertion into neuronal membranes. The ligands chosen for these comparisons were ^{3}H-raclopride and ^{3}H-SCH23390, 2 DA antagonists highly selective for the D_2 (Kohler et al., 1985) and D_1 (Iorio et al., 1983) sites, respectively.

Given the complexity of such a study, this report focuses on regions of the CNS whose anatomical circuitry is better understood, such as the olfactory bulb, hippocampus, and the basal ganglia, with minimal discussion of other regions of the rat forebrain and midbrain. The pituitary gland is also examined in detail, as this tissue contains a high density of D_2 receptors, and differences in receptor binding and mRNA distribution are unlikely to be due to the localization of D_2 binding sites on fibers. In addition to these anatomical considerations, several *in situ* hybridization and receptor binding controls were performed to ensure selectivity of hybridization and ligand binding.

Materials and Methods

Tissue preparation and incubation medium for receptor binding studies. Adult male Sprague-Dawley rats (Charles River, 200–250 gm) were sacrificed by decapitation, and their brains and pituitaries were quickly removed. Brains were frozen in liquid isopentane (−30°C) for 30 sec, while the pituitaries were frozen on crushed dry ice in Lipshaw M-1 embedding matrix. Frozen tissues were sectioned on a Bright cryostat (20 μm), thaw-mounted on precleaned and subbed microscope slides, and stored at −80°C. Immediately prior to using the tissue, the slide-mounted sections are gradually brought to room temperature and incubated (90 min, 22°C) with 200–400 μl of either the D_2-selective antagonist ^{3}H-raclopride (83.4 Ci/mmol, New England Nuclear) or the D_1-selective antagonist ^{3}H-SCH23390 (71.3 Ci/mmol, New England Nuclear) in 50 mM Tris buffer, pH 7.5 at 25°C, containing 0.1% ascorbic acid, 120 mM NaCl, 5 mM KCl, and 1 mM $MgCl_2$. As SCH23390 has been reported to bind serotinergic sites (5-HT_2), 1 μM ketanserin, a selective 5-HT_2 antagonist was added to all ^{3}H-SCH23390 binding studies.

Following a 90 min incubation period, the slides were drained, washed in 4 consecutive 250 ml, 50 mM Tris, pH 7.6 at 4°C, washes containing 0.1% ascorbic acid, 120 mM NaCl, 5 mM KCl, and 1 mM $MgCl_2$. Slides incubated with ^{3}H-raclopride were given four 2-min washes, while those labeled with ^{3}H-SCH23390 were given four 4-min washes. All slides were then quickly dipped in 250 ml distilled water (4°C) and dried with a portable hair dryer set to "cool." Nonspecific binding was evaluated by treating a parallel set of slides with the same concentrations of tritiated ligand with a 1 μM final concentration of an unlabeled competitor: spiperone to displace ^{3}H-raclopride and SCH23390 to displace ^{3}H-SCH23390.

Saturation studies. Prior to preparing tissue for receptor autoradiography, saturation experiments were performed on slide-mounted brain sections to determine the binding kinetics of ^{3}H-raclopride and ^{3}H-SCH23390. Forebrain sections were incubated with a minimum of 8 concentrations of either ^{3}H-raclopride (15.0–0.12 nM) or ^{3}H-SCH23390 (7.6–0.06 nM) and washed and dried as described earlier. The binding was quantified by placing brain sections in scintillation vials containing 10 ml of scintillant and vigorously shaking for 30 min in a metabolic shaker. Each data point is an average of 2 brain sections. Saturation experiments were performed at least twice and graphed as Scatchard plots. K_d and B_{max} values were determined with the LIGAND program developed by Munson and Rodbard (1980).

Competition studies. To characterize the binding sites labeled by ^{3}H-raclopride and ^{3}H-SCH23390, competition studies were performed with slide-mounted brain sections at concentrations 3 times the K_d value for each ligand. These concentrations correspond to the ones used in subsequent autoradiographic mapping studies and represent a 75% receptor occupancy for each ligand. Competition studies were performed with a series of dopaminergic compounds [haloperidol, chlorpromazine, spiperone, (+) and (−) butaclamol, droperidol, raclopride, and SCH23390], as well as nondopaminergic drugs (propranolol, clonidine, mianserin, and bremazocine). The brain sections were incubated, washed, and dried, and the binding was quantified as described earlier.

Autoradiographic mapping. After being brought to room temperature, slide-mounted sections were placed in incubation chambers and incubated with either ^{3}H-raclopride (5.7 nM) or ^{3}H-SCH23390 (4.4 nM). These concentrations correspond approximately to 3 times the K_d value for each ligand, producing an equivalent receptor occupancy. Following a 90 min incubation, the slides were washed and dried, as described above, and apposed to tritium-sensitive Hyperfilm (Amersham) for 2–4 weeks (^{3}H-SCH23390) or 4–8 weeks (^{3}H-raclopride). The Hyperfilm was exposed at room temperature, developed in Kodak D-19 (4 min, 19°C), agitated in 2% acetic acid (30 sec), fixed in Kodak Rapidfix (5 min), and washed under running water (30 min). Anatomical structures were determined using Nissl-stained sections in conjunction with the atlas of Paxinos and Watson (1986).

In situ *hybridization.* Slides adjacent to those used for autoradiographic mapping of D_1 and D_2 receptor binding sites were directly removed from storage at −80°C and placed into 4% formaldehyde for 60 min (22°C) prior to being processed for *in situ* hybridization (Sherman et al., 1986; Watson et al., 1987). Following three 5-min rinses in PBS, pH 7.4, sections were treated with proteinase K (1 μg/ml in 100 mM Tris, pH 8.0, 50 mM EDTA) for 10 min at 37°C. Slides were then rinsed in water, followed by 0.1 M triethanolamine, pH 8.0, and treated with a mixture of 0.1 M triethanolamine, pH 8.0, and acetic anhydride (400:1, vol/vol) with stirring for 10 min. The sections were then rinsed in 2 × SSC (300 mM NaCl, 30 mM sodium citrate, pH 7.2) for 5 min, dehydrated through graded alcohols, and allowed to air dry.

Brain sections were hybridized with ^{35}S-UTP-labeled riboprobes generated to the 495 *Sac I-Bgl II* fragment of a rat D_2 receptor (Bunzow et al., 1988). cRNA probes were diluted in hybridization buffer (75% formamide, 10% dextran sulfate, 3 × SSC, 50 mM Na_2PO_4, pH 7.4, 1 × Denhardt's, 0.1 mg/ml yeast tRNA, 0.1 mg/ml sonicated, denatured salmon sperm DNA, 10 mM dithiothrietol) to result in a final concentration of 2 × 10^6 dpm/30 μl. Volumes of 30 and 50 μl of diluted probe were applied to coronal and horizontal sections, respectively.

After hybridization (overnight, 55°C), the slides were rinsed in 2 × SSC (5 min) and treated with RNase A (200 μg/ml in 100 mM Tris, pH 8.0, and 0.5 M NaCl) for 30 min at 37°C. Subsequently, sections were rinsed in 2 × SSC for 10 min (22°C), 1 × SSC for 10 min (22°C), 0.5 × SSC at 55°C for 60 min, 0.5 × SSC at room temperature for 10 min, and finally dehydrated in graded alcohols and air-dried. Sections were then either exposed to Kodak XAR-5 X-Ray film for 1–3 d and developed, or dipped in Kodak NTB-2 emulsion and stored at 4°C for 6–17 d prior to development.

In situ *hybridization controls.* To ensure the specificity of the *in situ* hybridization signal, several control studies were performed. (1) The 495 bp cRNA probe used in the present study corresponds to the pu-

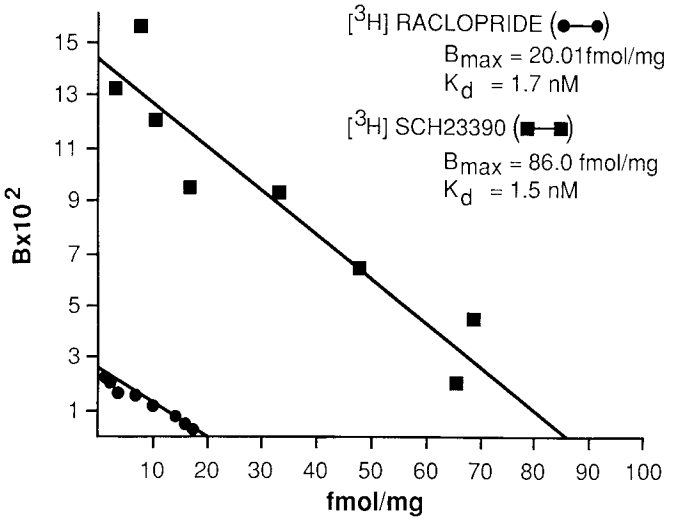

Figure 1. Scatchard plots of ^{3}H-raclopride and ^{3}H-SCH23390 binding in the rat forebrain. Note that each ligand appears to bind a single population of receptor sites and there are approximately 4 times as many D_1 sites (86 fmol/mg) as D_2 receptors (20 fmol/mg).

tative third cytosolic loop and the sixth and seventh transmembrane domains of the D_2 receptor. Given the homology of the sixth and seventh transmembrane domains to other G-protein coupled receptors, such a probe may potentially hybridize these receptors in addition to the D_2 receptor. To examine this issue, we performed *in situ* hybridization with a subcloned 205 bp fragment (EcoRI-Xho II) of the 495 bp clone that codes exclusively for the third cytosolic loop. A series of adjacent brain sections were hybridized either with the 205 bp or the 495 bp cRNA probes employing the same *in situ* conditions described above. (2) For RNase control, a series of paired, adjacent sections was divided into 2 sets: One slide from each pair was treated as described earlier for *in situ* hybridization, and the remaining slides from each pair were fixed in 4% formaldehyde and rinsed in PBS, but prior to treatment with proteinase K, were incubated with RNase A (200 μg/ml) for 30 min at 37°C. These slides were then processed as described in the *in situ* hybridization protocol. (3) For "sense"-strand control, another series of paired, adjacent sections was divided into 2 sets: One set was treated according to the *in situ* hybridization protocol, and the second set was treated identically, except that the cRNA used in the hybridization mixture was ^{35}S-UTP-labeled "sense"-strand RNA.

Results

Saturation studies

^{3}H-raclopride and ^{3}H-SCH23390 demonstrate saturable binding, and the results best fit a single-site model using the LIGAND program. As can be seen from Figure 1, ^{3}H-raclopride and ^{3}H-SCH23390 bound to a single population of sites with apparent affinity constants of 1.7 and 1.5 nM, respectively. The mean K_d values across multiple saturation studies are 2.2 nM for ^{3}H-raclopride and 1.55 nM for ^{3}H-SCH23390. While the affinities of these ligands for their respective binding sites appear similar, the relative abundance of each receptor varied markedly. In the forebrain slices used in the present study, there were 4 times as many D_1 sites (86.0 fmol/mg) as D_2 sites (20.0 fmol/mg) per milligram of tissue.

Competition studies

To characterize the pharmacological properties of each ligand, a series of competition studies was conducted. As can be seen from Table 1, ^{3}H-raclopride and ^{3}H-SCH23390 appear to selectively label D_2 and D_1 dopamine receptor sites, respectively.

Table 1. K_i concentrations (nM) of various compounds competing for the D_1 and D_2 receptor sites labeled with ^{3}H-SCH23390 (4.6 nM) and ^{3}H-raclopride (6.6 nM), respectively

	^{3}H-Raclopride	^{3}H-SCH23390[a]
(+)Butaclamol	1.19	227.47
(−)Butaclamol	>2506.0	>2463.0
Droperidol	3.41	>2463.0
Raclopride	5.34	>2463.0
Spiperone	5.35	>2463.0
Chlorpromazine	5.74	1037.72
Haloperidol	16.10	>2463.0
SCH23390	1157.58	2.58
Mianserin	1991.0	>2463.0
Clonidine	>2506.0	>2463.0
Bremazocine	>2506.0	>2463.0
Propranolol	>2506.0	>2463.0

[a] ^{3}H-SCH23390 binding was done in the presence of 1 μM ketanserin.

^{3}H-Raclopride binding was readily displaced by D_2 antagonists, including droperidol, spiperone, raclopride, chlorpromazine, and haloperidol. The binding was stereoselective with (+)butaclamol potently competing for the ^{3}H-raclopride site, and (−)butaclamol failing to displace it even at micromolar concentrations. SCH23390, a D_1 antagonist, and mianserin, a 5-HT_2 antagonist, were unable to effectively compete at the site labeled by ^{3}H-raclopride. Similarly, clonidine (α_2-adrenergic agonist), bremazocine (opioid) and propranolol (α- and β-adrenergic antagonist) failed to displace the binding at this site. Taken together, these results suggest that ^{3}H-raclopride binds selectively to D_2 dopaminergic receptor sites.

^{3}H-SCH23390 in the presence of 1 μM ketanserin appears to selectively label D_1 receptor sites. Of the compounds tested, only SCH23390 and (+)butaclamol displaced ^{3}H-SCH23390 (Table 1). Compounds such as (−)butaclamol, haloperidol, droperidol, raclopride, spiperone, mianserin, clonidine, bremazocine, and propranolol failed to compete for the sites labeled by ^{3}H-SCH23390. Chlorpromazine did displace ^{3}H-SCH23390, but required micromolar concentrations. The relative difference in potency between (+)butaclamol and its negative enantiomer suggests that the ^{3}H-SCH23390 binding is stereoselective.

Anatomical distribution

Consistent with the saturation results, autoradiographic studies suggest that D_1 binding sites are more densely distributed than D_2 sites in most of the rat CNS. In addition, D_1 receptors are more widely distributed and are observed at all levels of the neuraxis, while D_2 receptor sites are densely distributed primarily in the basal ganglia, olfactory bulb, and pituitary. By comparison, the distribution of D_2 receptor mRNA more closely corresponds to the D_2 binding sites labeled with ^{3}H-raclopride than the D_1 sites demonstrated with ^{3}H-SCH23390.

The following is a qualitative comparison of the distribution of the D_2 receptor mRNA in relation to the dopaminergic ligand binding sites. The level of mRNA or receptor binding in caudate-putamen is used for comparison with other brain regions and pituitary. The descriptions are also within a ligand or mRNA distribution, so that an area described as dense for D_2 binding sites, for example, may be equivalent to an area of moderate D_1 receptor binding on the basis of receptor number. The em-

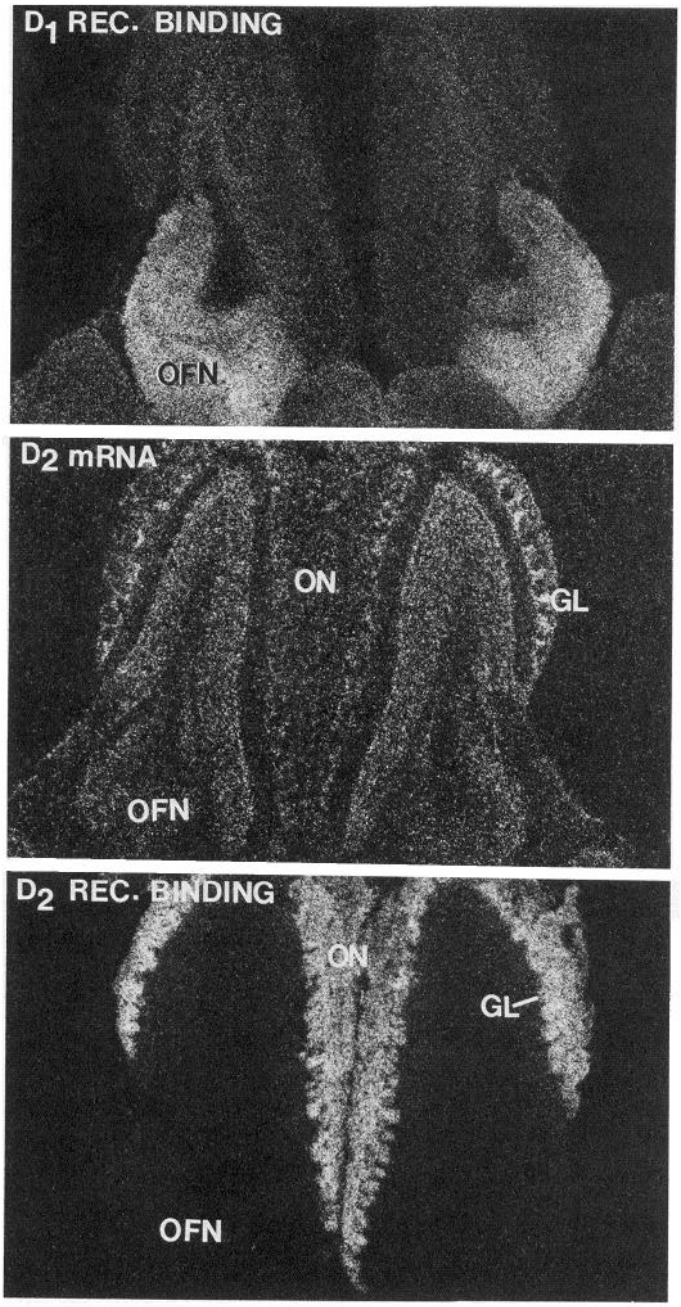

Figure 2. Dark-field autoradiograms comparing D_1 and D_2 receptor binding to the distribution of D_2 mRNA in horizontal sections of olfactory bulb. D_2 receptor binding is observed in the olfactory nerve layer (*ON*) and the glomerular layer (*GL*). D_2 receptor mRNA, by comparison, can be visualized in the periglomerular cells of GL, olfactory nucleus (*OFN*) and the internal granular layers. D_1 sites are predominant only in the olfactory nucleus.

phasis of this study is not to quantify receptor mRNA and binding levels, but to compare their anatomical distributions. Detailed quantitative distribution studies of D_1 and D_2 receptors have been published elsewhere (Boyson et al., 1986; Dawson et al., 1986; Bouthenet et al., 1987; Charuchinda et al., 1987; Joyce and Marshall, 1987).

Telencephalon

With its precise laminations, the olfactory bulb is a region where D_1 and D_2 receptor sites can be easily differentiated. D_2 binding sites are restricted to the olfactory nerve layer (ON) and glomerular cell layer (GL) where they are densely distributed (Fig. 2). By comparison, D_2 receptor mRNA can be visualized in the olfactory nucleus, glomerular, and internal granular cell layers. Within the glomerular layer, D_2 mRNA is restricted to the periglomerular cells whose processes extend into the glomerula. In contrast, D_1 sites are not prominent in the olfactory bulb, with a light amount of binding observed in the glomerular, plexiform, and internal granular layers. Higher levels of D_1 receptors are seen in the olfactory nucleus, where no D_2 binding sites are observed.

Within the cortical fields, D_2 receptor binding is densest in the entorhinal cortex. Layer I of entorhinal cortex shows fairly dense D_2 binding, with no observable binding in layer II and moderate amounts in layer III. Only a very light density of ^{3}H-raclopride binding is seen in the cingulate, frontal, parietal, and temporal cortices, being restricted primarily to deeper layers. A light density of D_2 receptors can also be visualized in the piriform cortex. By comparison, dense levels of D_2 receptor mRNA are found in the superficial aspects of layer I and in layers II–III of the frontal, parietal, and temporal cortex. Deeper layers (V, VI) of cingulate, frontal, parietal, and temporal cortex show moderate to low levels of D_2 receptor mRNA. Within paleocortical regions, entorhinal cortex (layers II–III) and the most superficial cells of layer I demonstrate dense levels of D_2 receptor mRNA. Similarly, piriform cortex shows a high density of D_2 receptor mRNA. In contrast to D_2 binding, D_1 receptor sites are more abundant and widely distributed throughout neo- and paleocortex. Moderate densities of D_1 receptor sites are seen in deep layers of cingulate, frontal, parietal, and temporal cortices, with light diffuse labeling observed in more superficial layers. Within the paleocortex, moderate amounts of D_1 binding are seen in the piriform cortex, with D_1 binding restricted to layer I of entorhinal cortex.

Of the telencephalic regions examined, the caudate-putamen contains the highest density of D_2 receptor mRNA and D_1 and D_2 receptor binding sites. The distribution of D_2 binding sites appears to be heterogeneous with this structure, with the highest densities in the dorsomedial tips and the dorso- and ventrolateral aspects of this nucleus (Fig. 3). D_2 receptor binding extends into the ventral striatum and is particularly dense in the rostral part of the nucleus accumbens, as well as in the olfactory tubercle. Somewhat reduced levels of ^{3}H-raclopride binding are seen in the caudal two-thirds of the nucleus accumbens, where the binding appears to be less dense than in the caudate-putamen (Fig. 3).

D_1 receptor sites are also densely distributed in the caudate-putamen, with a similar medial–lateral receptor gradient. The dopaminergic receptors differ in the nucleus accumbens, however, where D_1 sites are dense throughout this nucleus, with particularly high levels observed in the shell of the accumbens (Fig. 3). D_1 receptor binding extends ventrally and is dense throughout the olfactory tubercle.

In contrast to the heterogeneous D_2 ligand distribution, D_2 receptor mRNA is uniformly distributed in the caudate-putamen (Fig. 3). D_2 receptor mRNA levels are also dense in the nucleus accumbens, where the levels appear equivalent to those seen in the caudate-putamen, making the 2 structures appear as a single unit. More ventrally, the olfactory tubercle contains one of the highest concentrations of D_2 receptor mRNA.

Within the septum, the lateral and medial nuclei demonstrate a light density of D_2 binding. D_2 receptor mRNA shows a similar

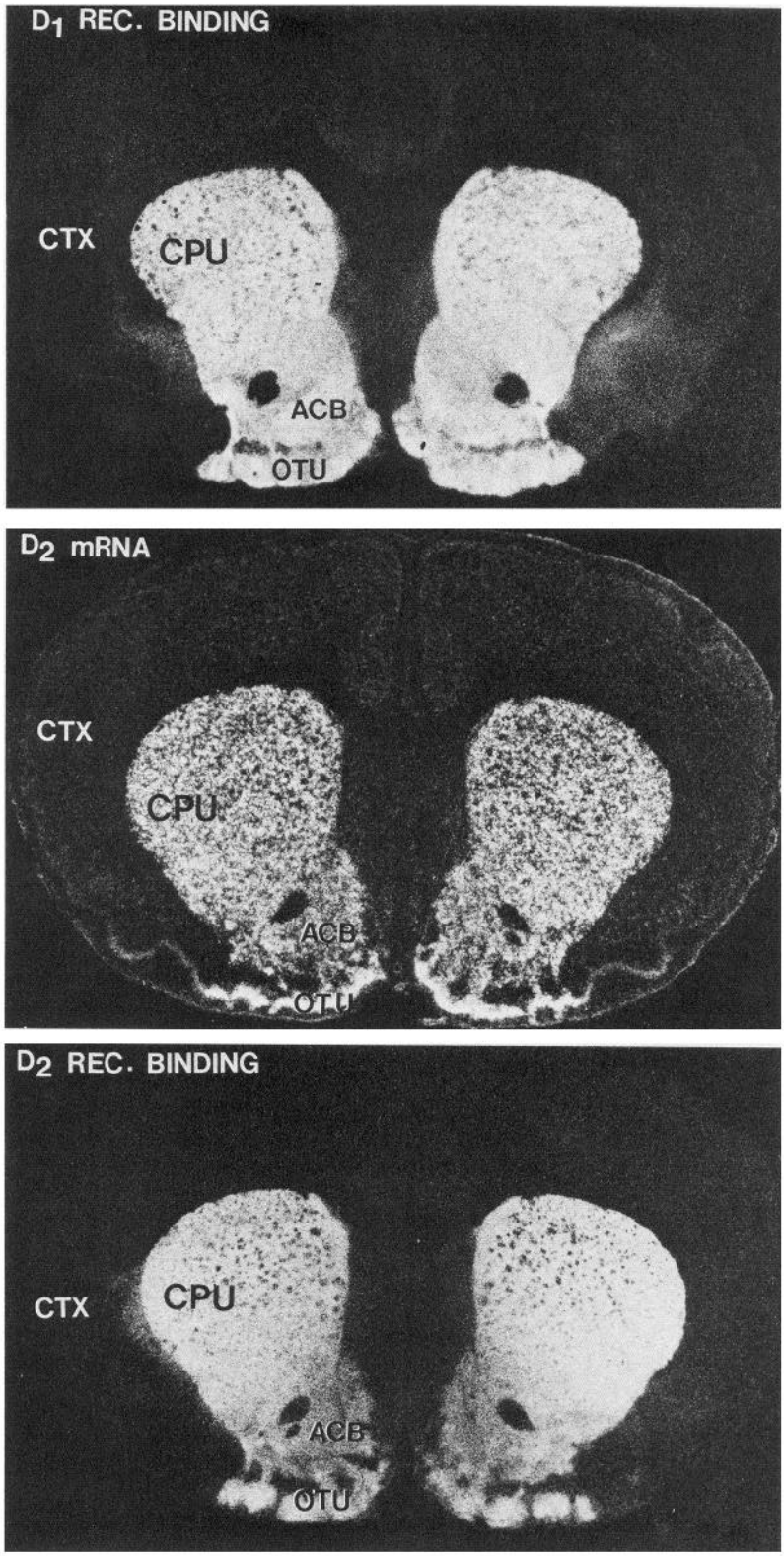

Figure 3. Dark-field autoradiograms of D_1 receptor binding and D_2 receptor mRNA and ligand binding. Note the high levels and good correspondence of D_2 receptor mRNA and dopamine receptor binding in the caudate-putamen (*CPU*), nucleus accumbens (*ACB*), and olfactory tubercle (*OTU*). There appears to be a lack of correspondence between the distributions of D_2 binding sites and D_2 receptor mRNA in the superficial layers of cortex (*CTX*).

distribution, with a relatively low level of D_2 receptor mRNA found in these nuclei. D_1 binding sites can also be localized in the septum, but these sites are predominantly in the lateral nucleus.

The globus pallidus, a major efferent target of the caudate-putamen, shows D_1 and D_2 ligand binding, as well as D_2 receptor mRNA (Fig. 4). The level of D_2 ligand binding in this region is fairly light, appearing densest in the lateral portion of the nucleus. By comparison, cells containing D_2 receptor mRNA appear widely distributed throughout the globus pallidus and appear densely labeled under these hybridization conditions. As can be appreciated from Figure 4, given the high amounts of

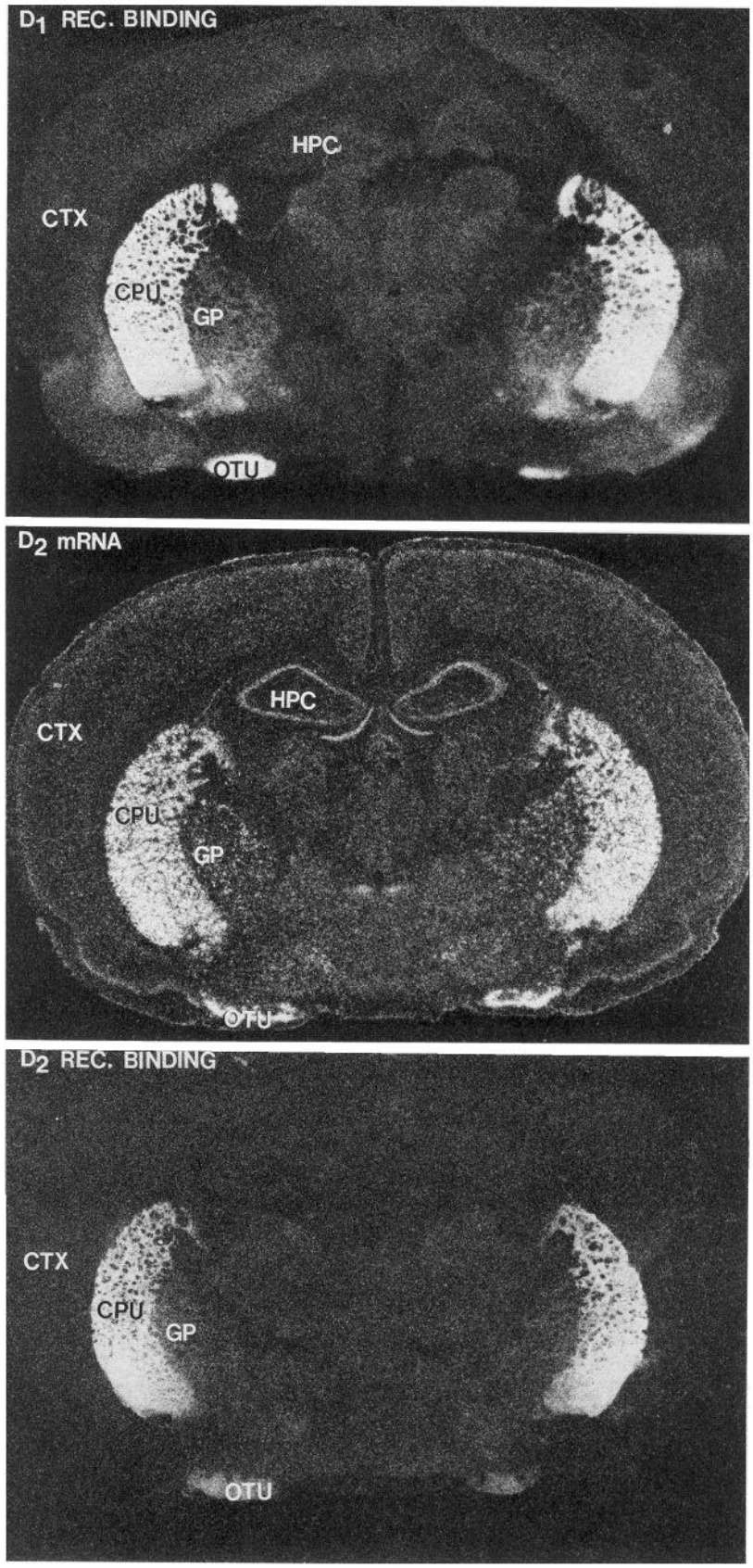

Figure 4. Dark-field autoradiograms of D_1 and D_2 receptor binding as compared to D_2 receptor mRNA localization. D_2 receptor mRNA and D_1 and D_2 binding sites can be visualized in the caudate-putamen (*CPU*), globus pallidus (*GP*), and olfactory tubercle (*OTU*). Note that single-cell resolution can be attained in the globus pallidus in the visualization of D_2 receptor mRNA.

D_2 receptor mRNA and the wide distribution of these positive cells, individually labeled pallidal cells can be resolved even at this low magnification. Cells showing D_2 receptor mRNA appear more numerous in the dorsal portion of the globus pallidus and become more widespread ventrally. D_2 receptor mRNA can also be visualized in the ventral pallidum, but the apparent density of labeled cells is not as great as observed in the globus pallidus. Moderate densities of D_1 binding sites can also be observed in the globus pallidus, with dense levels seen in the ventral pallidum.

The amygdala, a region where D_1 and D_2 receptor sites can be differentiated, demonstrates little or no D_2 ligand binding in most of the amygdaloid nuclei, with only a light labeling in the medial nucleus. In contrast, D_1 receptor sites are densely distributed throughout most of the amygdala, including the cortical, lateral, and basalateral nuclei, with moderate densities seen in the medial nucleus. By comparison, light levels of D_2 receptor mRNA can be visualized in the lateral and basolateral nuclei, with somewhat higher levels observed in the medial nucleus.

The hippocampal formation with its laminated structure is an excellent tissue for comparing receptor binding and mRNA distributions. Within the hippocampus, D_2 receptor binding is restricted to the stratum lacunosum moleculare and subiculum, where a light to moderate density of binding is observed (Fig. 5). D_2 receptor mRNA, on the other hand, is seen in the pyramidal cell layer (CA1, CA2, CA3) and in the granular cells of the dentate gyrus. For comparison, moderate densities of D_1 receptors are observed in the dentate gyrus, with low densities in the stratum moleculare and oriens.

Diencephalon

Compared to the telencephalon, far fewer regions of the diencephalon demonstrate D_2 receptor binding or mRNA. Within the thalamus, the medial and lateral habenula and the zona incerta have particularly high amounts of D_2 receptor mRNA (Fig. 6). By comparison, D_2 and D_1 binding can be seen in the lateral habenula, but does not appear to be present in the medial habenula and zona incerta.

In the hypothalamus, D_2 receptor mRNA is restricted to the anterior and lateral hypothalamic areas, lateral mammillary nucleus, and the paraventricular and ventromedial nuclei, where moderate to low levels are observed. D_2 receptor binding appears diffuse and light throughout most of the hypothalamus, including the lateral, dorsomedial, ventromedial, and arcuate nuclei. The lateral mammillary nucleus appears to be the exception, with densely localized D_2 binding sites and mRNA (Fig. 7). D_1 binding sites are lightly distributed throughout most of the hypothalamus, including the lateral, ventromedial, and arcuate nuclei, with only the suprachiasmatic nucleus demonstrating a high density of D_1 sites.

Mesencephalon

Of the mesencephalic structures, the substantia nigra (SN) and ventral tegmental area (VTA) have the highest densities of dopaminergic receptor binding and D_2 receptor mRNA. D_2 ligand binding is predominantly in the pars compacta, with light labeling in the pars reticulata (Fig. 7). Consistent with this localization, D_2 receptor mRNA is restricted to the cells of the pars compacta, with large cells in the pars reticulata occasionally labeled. D_2 receptor binding and mRNA appear to show a similar distribution in the VTA, where a moderate density of D_2

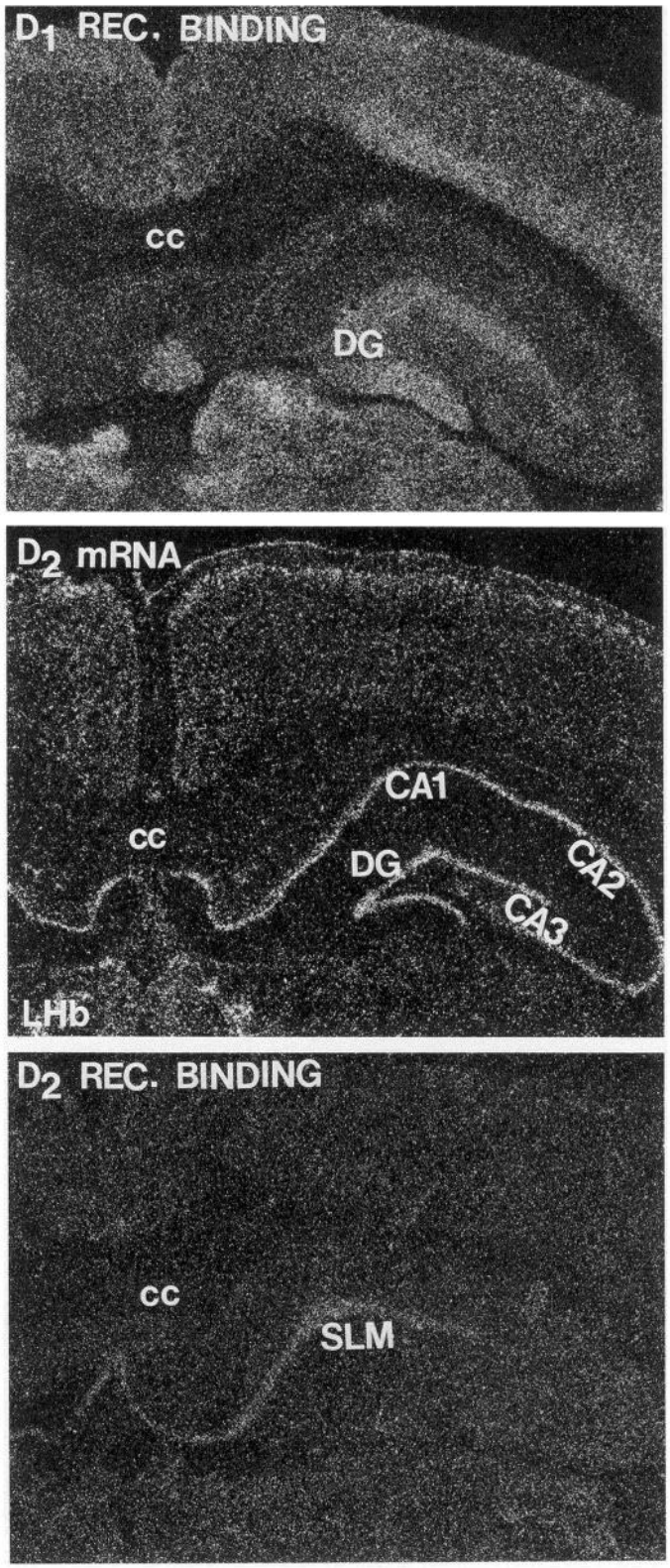

Figure 5. Dark-field autoradiograms of D_1 and D_2 receptor binding as compared to D_2 receptor mRNA in the hippocampus. D_2 receptor mRNA can be visualized in the pyramidal cell layer (*CA1, CA2, CA3*) of the hippocampal formation and in the granular cells of the dentate gyrus (*DG*). D_2 receptor binding, on the other hand, is restricted to the stratum lacunosum moleculare (*SLM*), while D_1 binding is observed in the dentate gyrus and in stratum moleculare and oriens. Other abbreviations: *cc,* corpus callosum; *LHb,* lateral habenula.

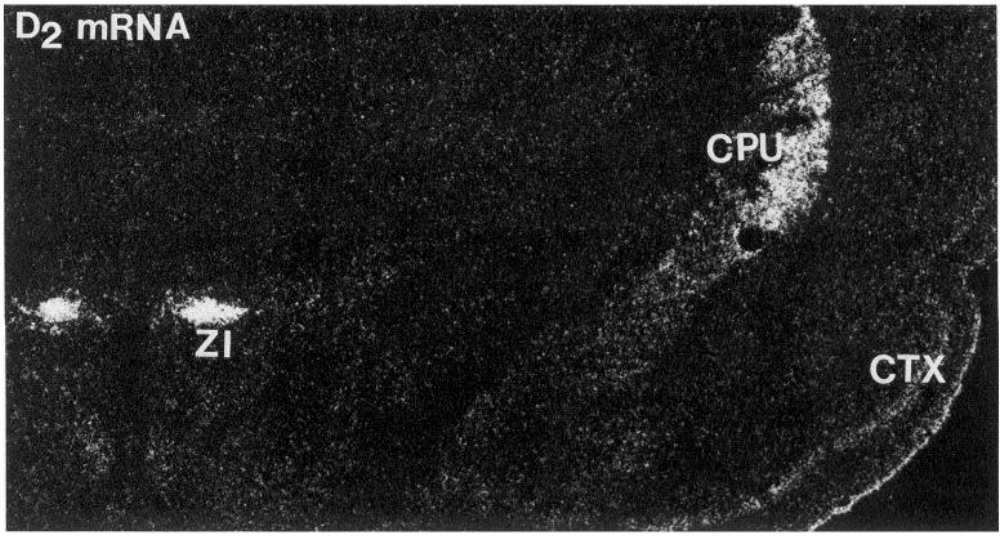

Figure 6. Dark-field autoradiogram of a D_2 receptor mRNA at the level of the diencephalon. Note the high levels of D_2 receptor mRNA in the zona incerta (*ZI*), caudate-putamen (*CPU*), and cortex (*CTX*).

binding and high levels of D_2 receptor mRNA can be observed. In contrast, D_1 receptor binding sites are localized predominantly in the pars reticulata of the substantia nigra, with moderate densities extending into the VTA. Horizontal sections illustrating the distributions of D_1 and D_2 receptors in relation to D_2 receptor mRNA in the basal ganglia are presented in Figure 8.

More rostrally in the quadragemini, moderate amounts of D_2 receptor mRNA can be visualized in the inferior colliculus, while little, if any, D_2 receptor mRNA can be seen in the superior colliculus. In contrast, moderate levels of D_2 binding and high densities of D_1 sites are present in the superficial gray layer of the superior colliculus. This relationship is somewhat reversed in the inferior colliculus, where moderate amounts of D_2 receptors are present and only light densities of D_1 sites are found. Other mesencephalic regions, such as the periquaductal gray area, raphe nuclei, and interpeduncular nucleus show light to moderate levels of D_2 receptor mRNA, and D_1 and D_2 binding.

Pituitary gland

D_2 receptor binding is very dense in the intermediate lobe of the pituitary, with light labeling in the anterior lobe (Fig. 9). D_2 receptor mRNA shows a corresponding distribution with high levels of mRNA observed in the intermediate lobe and individually labeled cells in the anterior lobe. In contrast, D_1 receptors are restricted to the neural lobe, where there is a light density of binding sites.

In situ *controls*

Comparison of sections hybridized with the 205 bp EcoRI-Xho II probe, which is directed exclusively to the third cytosolic loop, to the longer 495 bp probe, demonstrated that the 2 cRNA probes labeled the same brain structures (Fig. 10), suggesting the 495 bp probe does not cross-hybridize to other G-protein coupled receptors. As can be seen from Figure 10, given the higher specific activity of the 495 bp probe, the quality of the *in situ* signal is improved over the shorter 205 bp cRNA probe.

No specific hybridization was observed in any of the brain areas identified following either RNase pretreatment or "sense"-strand hybridization. Direct comparisons of brain sections with and without RNase pretreatment, or following "sense" and "antisense" hybridization, are illustrated in Figure 11.

Discussion

In agreement with previous receptor autoradiographic studies (Boyson et al., 1986; Dawson et al., 1986; Bouthenet et al., 1987; Charuchinda et al., 1987; Richfield et al., 1987; Wamsley et al., 1989), D_1 and D_2 receptor sites are differentially distributed in the CNS and pituitary. D_1 receptors show a widespread distribution, with binding observed in the basal ganglia, neocortical and paleocortical regions, amygdala, hippocampus, thalamus, and the neural lobe of the pituitary. In contrast, the distribution of D_2 binding sites appears restricted primarily to the olfactory bulb, basal ganglia, and the intermediate lobe of the pituitary. Given these distinct receptor binding patterns, the distribution of D_2 receptor mRNA generally corresponds to the D_2 receptor binding sites labeled by ^{3}H-raclopride. These findings support previous dopamine receptor binding studies in cells transfected with a full length DNA coding for the D_2 receptor (Bunzow et al., 1988) and extend these findings to the CNS.

Good correspondence between the distributions of D_2 receptor mRNA and ligand binding can be seen in the caudate-putamen, nucleus accumbens, olfactory tubercle, globus pallidus, lateral mammillary nucleus, substantia nigra, ventral tegmental area, and pituitary gland. Despite such concordance, subtle differences can be seen in the precise localization of the mRNA and binding site even at this level of analysis. For example, within the caudate-putamen D_2 receptor binding is heterogeneously distributed, being densest in the lateral extent of the nucleus, while the distribution of D_2 receptor mRNA appears relatively homogeneous and does not demonstrate a mediolateral gradient. This difference may be due to the localization of D_2 binding sites on cortical projections to the caudate-putamen (e.g., Schwarcz et al., 1978), which would affect the D_2 ligand binding distribution, but not the mRNA localization within the striatum. Similar subtle differences can be seen in the globus pallidus, where D_2 receptor binding is lightly and diffusely distributed, while *in situ* studies demonstrate distinctly labeled pallidal cells. Here too, the difference may be more apparent than real, as the binding sites are likely on pallidal fibers and terminals, while the D_2 receptor mRNA is localized to the cell bodies of widely distributed pallidal neurons.

While D_1 receptor binding sites can be observed in many of

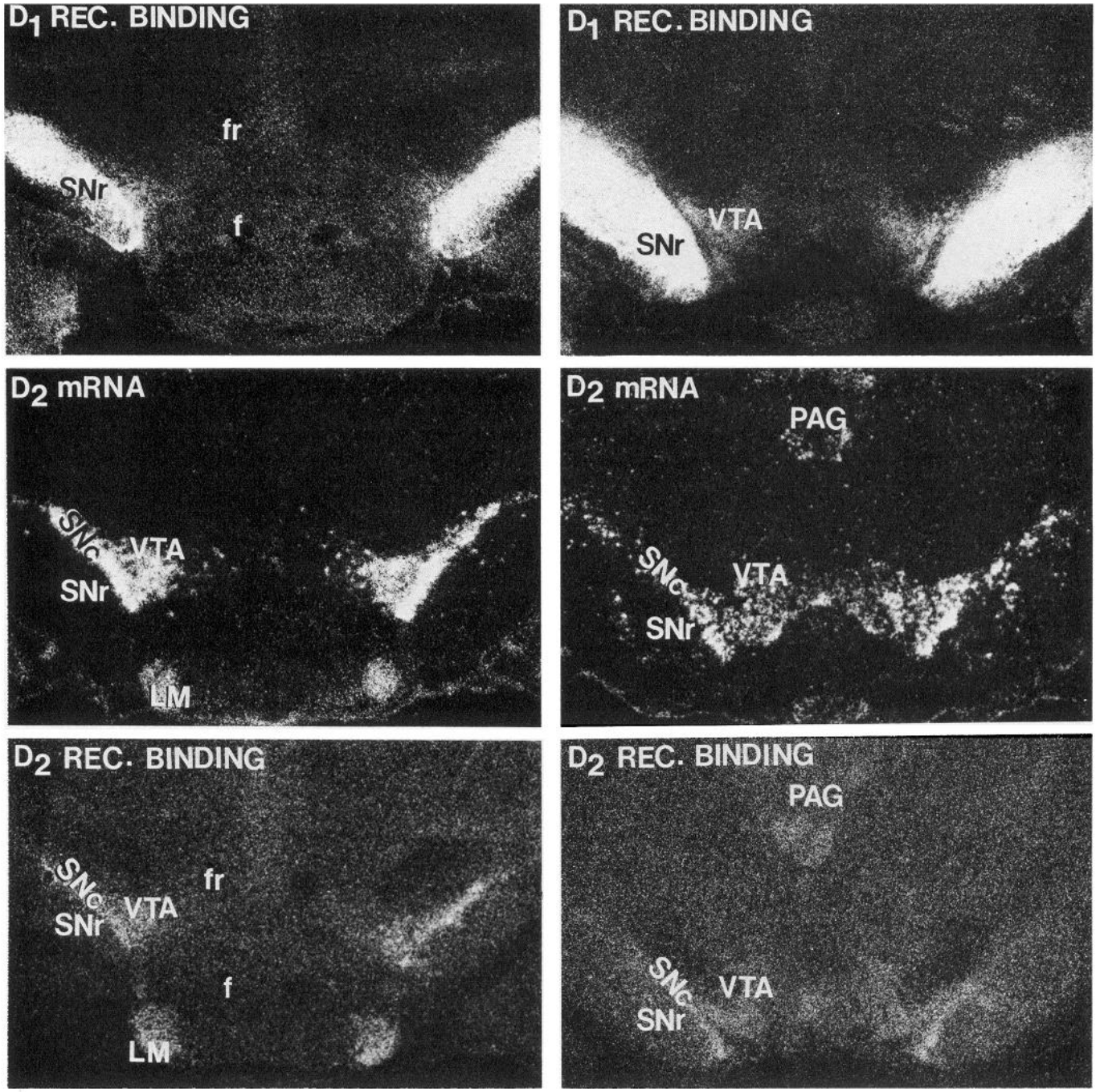

Figure 7. Dark-field autoradiograms of D_1 and D_2 receptor binding as compared to D_2 receptor mRNA at 2 levels of the substantia nigra. A good correspondence between the localization of D_2 binding sites and mRNA can be seen in the substantia nigra, pars compacta (*SNc*), ventral tegmental area (*VTA*), and lateral mammillary nucleus (*LM*). In contrast, D_1 receptor sites can be observed in the substantia nigra, pars reticulata (*SNr*), with little or no binding seen in the lateral mammillary nucleus. Other abbreviations: *f,* fornix; *fr,* fasciculus retroflexus; *PAG,* periaquaductal gray.

the same structures that also express D_2 receptors (e.g., caudate-putamen, nucleus accumbens, globus pallidus, substantia nigra, and pituitary), their precise distribution often varies markedly from the D_2 receptor mRNA and binding sites. For example, in the substantia nigra, D_1 receptor binding is localized in the pars reticulata, while D_2 receptor mRNA and binding is observed primarily in the pars compacta. Similarly, in the pituitary, D_1 sites are restricted to the neural lobe, while D_2 receptor mRNA and binding are seen in the intermediate and anterior lobes. A final example is the lateral mammillary nucleus, where D_2 receptors are fairly dense and little or no D_1 receptors are observed. In other regions where there is a high density of both D_1 and D_2 receptor sites, such as the caudate-putamen, nucleus accumbens, and olfactory tubercle, determining whether the D_2 receptor mRNA distribution corresponds better to a D_1 or D_2 receptor pattern is difficult.

Despite the overall good correspondence between the distribution of D_2 receptor mRNA and D_2 ligand binding, there are

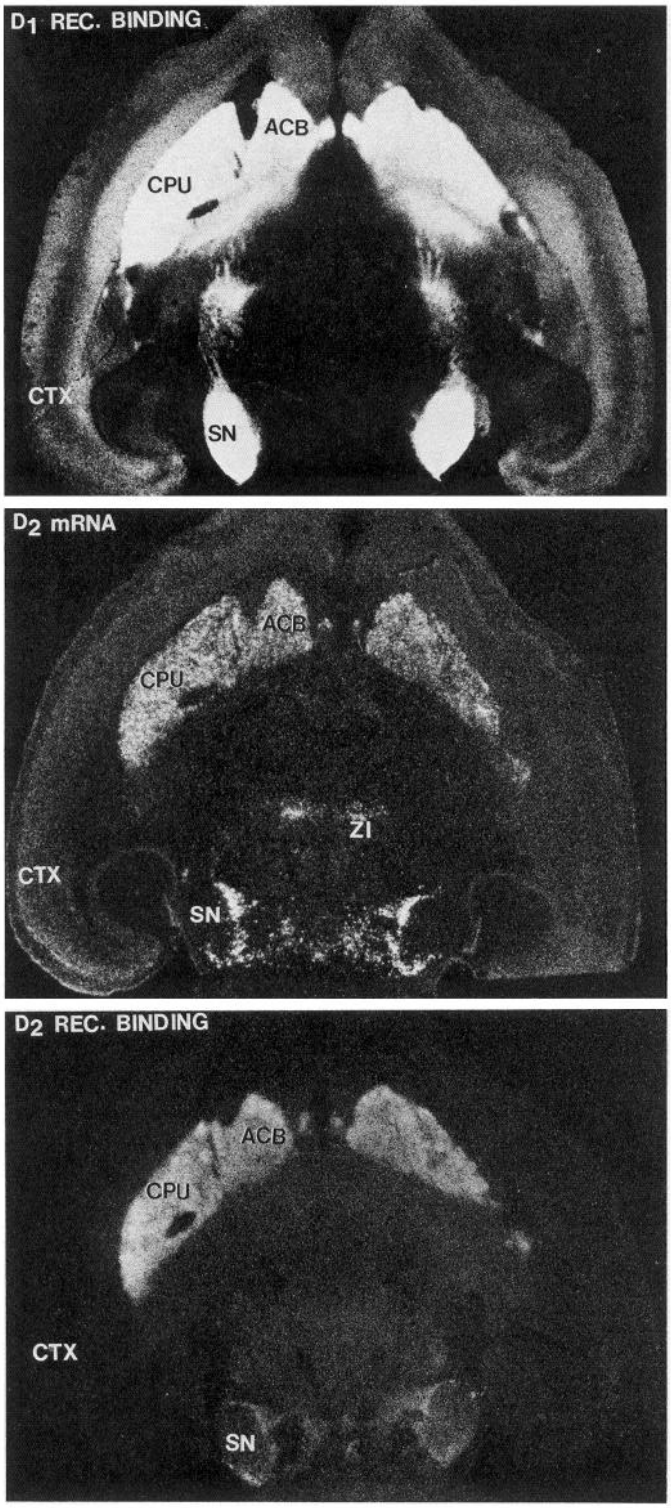

Figure 8. Dark-field autoradiogram of horizontal rat brain sections showing the distributions of D_2 receptor mRNA and D_1 and D_2 receptor binding. Note the good correspondence in the localization of D_2 binding sites and mRNA in the caudate-putamen (*CPU*), nucleus accumbens (*ACB*), and substantia nigra (*SN*). Regions where there is a lack of correspondence between D_2 binding and mRNA include cortex (*CTX*), hippocampus, and zona incerta (*ZI*).

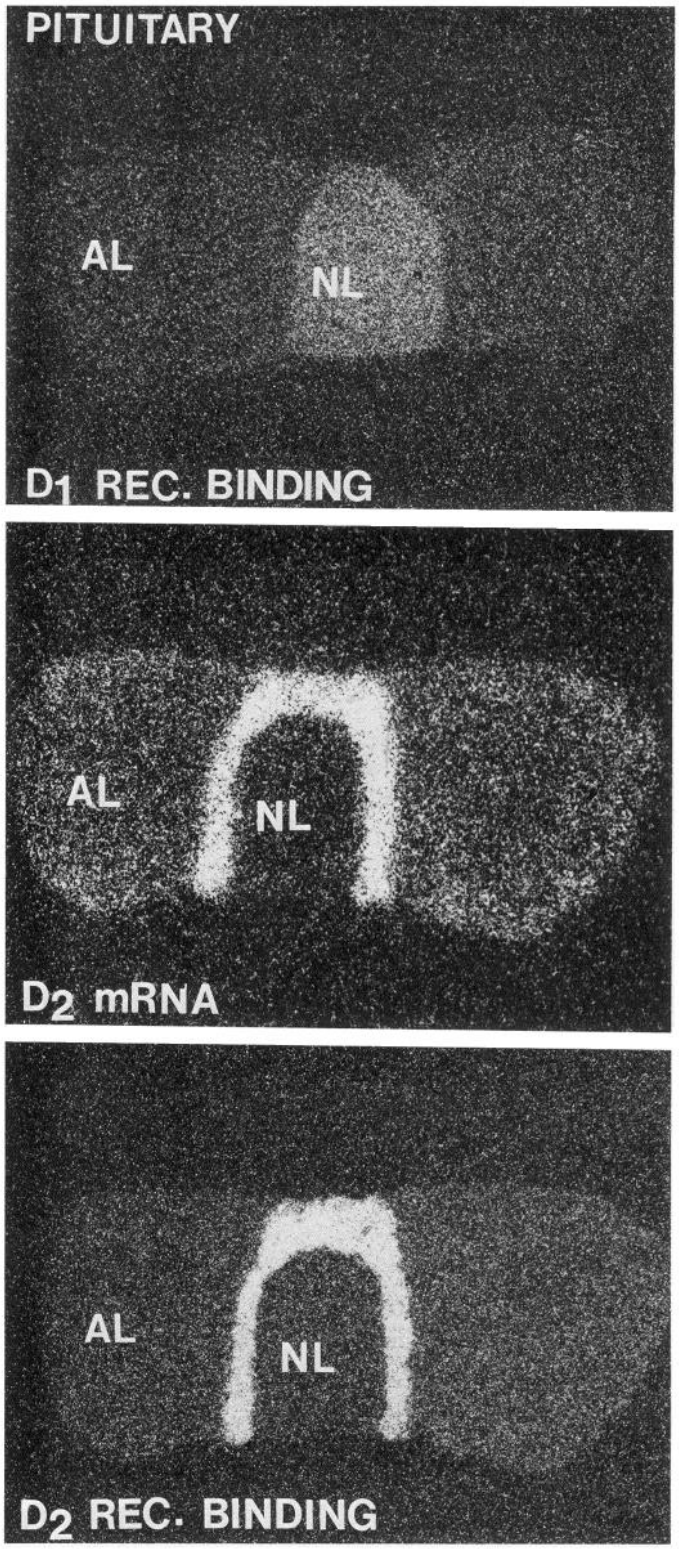

Figure 9. Dark-field autoradiograms of D_1 and D_2 receptor binding in the rat pituitary as compared to the distribution of D_2 receptor mRNA. Note the high levels of D_2 receptor mRNA and ligand binding in the intermediate lobe and the light labeling in the anterior lobe (*AL*). D_1 binding sites, in contrast, are restricted to the neural lobe (*NL*).

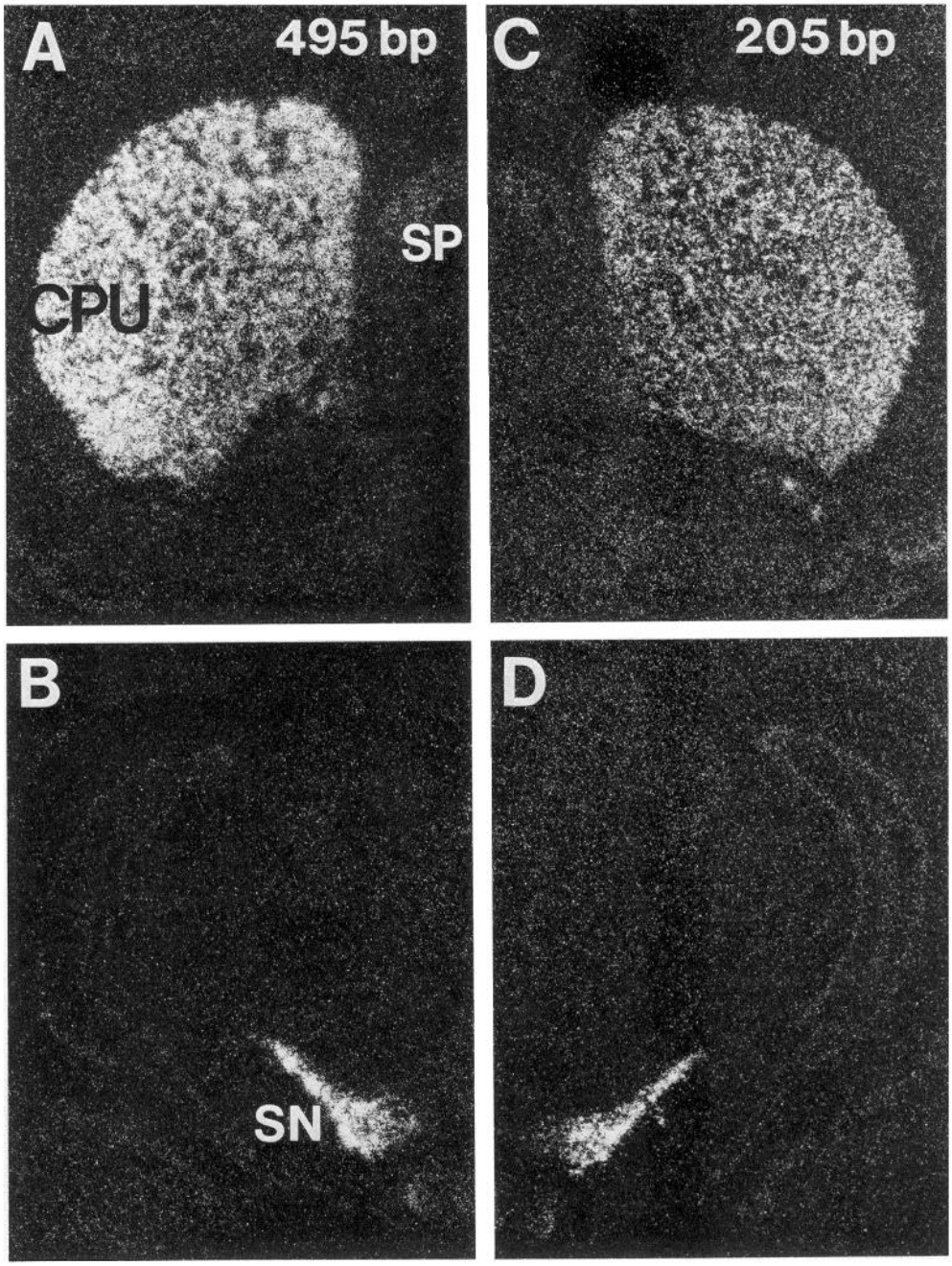

Figure 10. Comparison of adjacent telencephalic and mesencephalic sections hybridized to either the 495 bp probe (*A* and *B*) or the 205 bp probe (*C* and *D*). The dark-field images demonstrate that the same brain regions are labeled with each probe, suggesting that the longer 495 bp probe is not cross-hybridizing with other 7 transmembrane receptors. Note also that, because of its higher specific activity, the 495 bp probe produces a better quality *in situ* signal. Abbreviations; *CPU,* caudate-putamen; *SN,* substantia nigra; *SP,* septum.

a number of brain areas that demonstrate a lack of correspondence. These include the neocortex, zona incerta, olfactory bulb, and hippocampus. While it is at present difficult to determine the precise reason for this discrepancy, several possible explanations may be applicable depending on the anatomical region involved.

One possible explanation for a lack of correspondence in some brain regions between receptor binding and mRNA distributions may be inherent technical limitations. The visualization of D_2 receptor mRNA with S^{35}-labeled riboprobes may be a more sensitive means of detecting dopaminergic receptors than is possible with receptor autoradiography with ^{3}H-labeled ligands. In addition, differential quenching of the 2 isotopes may contribute subtle differences in grain distributions.

Other technical problems may be methodological, such as the undesired labeling of other receptor mRNAs or binding sites. However, the *in situ* hybridization controls of RNase pretreatment and "sense-strand" labeling would argue that there is specific hybridization. Further, *in situ* hybridization with the 205 bp cRNA probe that has no sequence identity to any other cloned receptor results in the same mRNA distribution as observed with the longer 495 bp probe. We have used the 495 bp for this mapping study because of the higher specific activity that can be achieved, thereby enhancing the sensitivity and quality of the *in situ* procedure.

With regards to the receptor binding data, ^{3}H-raclopride and ^{3}H-SCH23390 have been reported to be highly selective ligands for the D_2 and D_1 receptor sites, respectively (Iorio et al., 1983; Billard et al., 1984; Kohler et al., 1985), and the competition results generated under the autoradiographic conditions used in

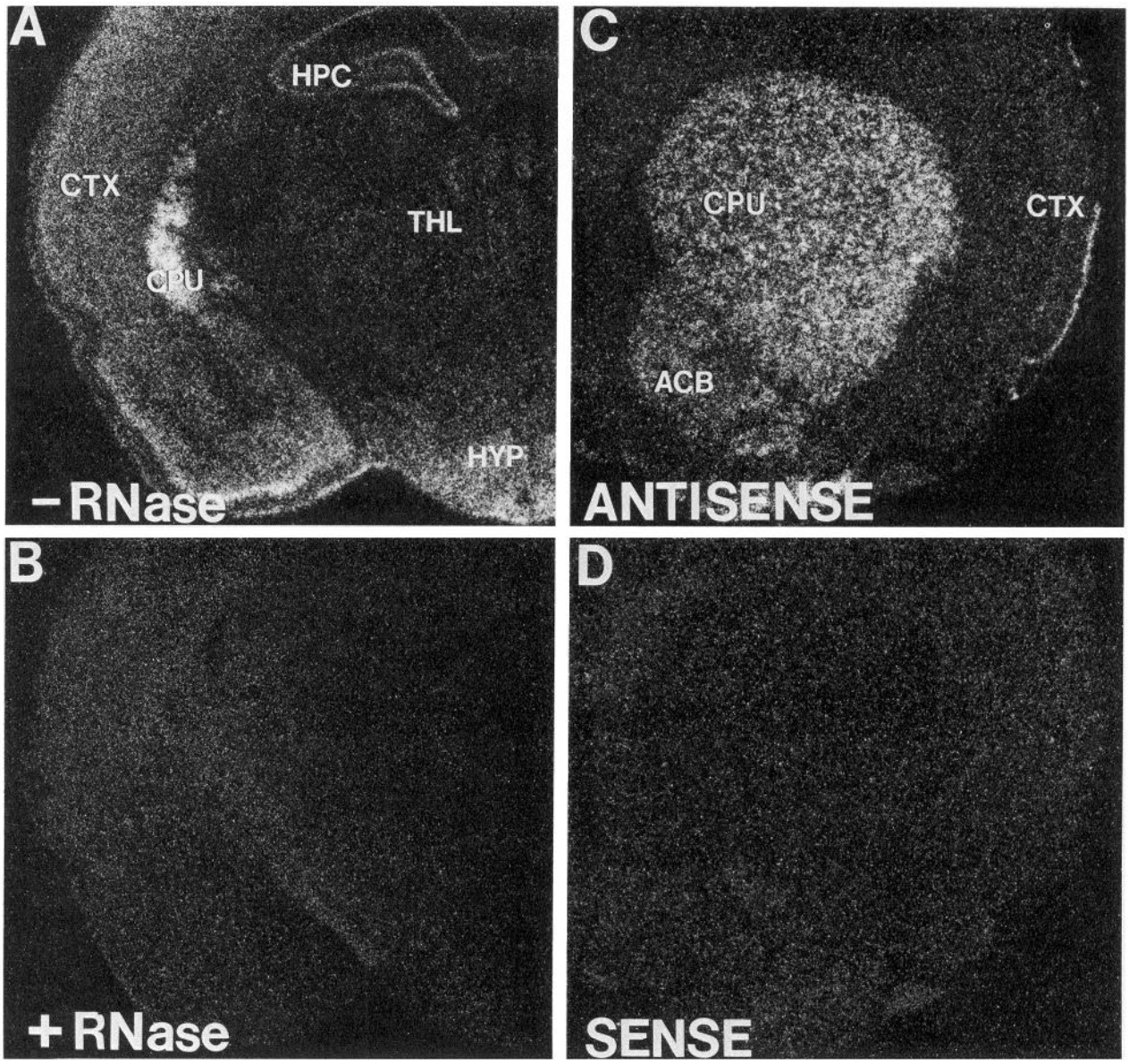

Figure 11. *In situ* controls. *A* and *B* compare adjacent slides that were either treated with RNase A (30 min, 37°C) (*B*) or not treated (*A*) prior to *in situ* hybridization. *C* and *D* compare a second set of adjacent sections hybridized with either "antisense" (*C*) or "sense" (*D*) cRNA probes. Note that neither RNase pretreatment nor hybridization with a "sense"-strand cRNA produced a specific signal. Abbreviations: *ACB,* nucleus accumbens; *CPU,* caudate-putamen; *CTX,* cortex; *HPC,* hippocampus; *HYP,* hypothalamus; *THL,* thalamus.

the present study are in full agreement with these conclusions. ^{3}H-Raclopride is stereoselectively displaced by D_2 antagonists [e.g., (+)butaclamol, haloperidol, spiperone], while compounds such as (−)butaclamol, clonidine, bremazocine, or propranolol fail to displace this ligand. Similarly, binding sites labeled by ^{3}H-SCH23390 are only displaced by unlabeled SCH23390, and at higher concentrations, (+)butaclamol and chlorpromazine.

While technical limitations may contribute to a lack of correspondence, they cannot explain the marked differences in D_2 receptor binding and mRNA distributions observed in some brain regions. Discordance in the distributions may be due to presence of D_2 receptor mRNA and no receptor binding or the converse of D_2 receptor binding and no D_2 receptor mRNA. The zona incerta and neocortex are examples of regions which demonstrate receptor mRNA and little or no D_2 receptor binding, suggesting that the D_2 receptor is translated and transported to sites distant from the point of transcription. The zona incerta, for example, projects to the lateral septum and hypothalamus, where D_2 receptor binding can be observed.

The olfactory bulb and hippocampus provide the converse example of the presence of D_2 receptor binding and no D_2 receptor mRNA. In the olfactory bulb, D_2 receptor binding is dense in the olfactory nerve layer (ON) and glomerular layer (GL), while D_2 receptor mRNA is found in the periglomerular cells of GL and in the internal granular layer. The lack of D_2 receptor mRNA in the ON is because this layer is composed of densely packed unmyelinated axons originating from the olfactory receptors. Similarly, the presence of D_2 receptor mRNA in the periglomerular cells and D_2 ligand binding in the glomerular cells would suggest that D_2 receptors may be synthesized in the

periglomerular cells and transported down their dendritic projections (Halasz and Shepherd, 1983) to the glomerular cells.

A similar pattern may be observed in the hippocampus, where D_2 receptor mRNA is localized in the pyramidal cell layer of the hippocampal formation and the granular cells of the dentate gyrus, while D_2 receptor binding is restricted to the stratum lacunosum moleculare. The pyramidal cells of the hippocampus and granular cells of the dentate gyrus are oriented with their apical dendrites synapsing in the stratum lacunosum moleculare, so that the D_2 binding protein may be synthesized in these cells and transported to this dendritic field. This scenario would imply that there is a mechanism involved to direct the transport of the nascent receptor from the site of translation to the point of its subsequent insertion in the membrane. While such an explanation is appealing, it cannot be determined at present whether the D_2 receptor binding observed in the stratum lacunosum moleculare is not from an extrahippocampal projection, such as the entorhinal cortex.

Recent studies (Dal Toso et al., 1989; Giros et al., 1989; Monsma et al., 1989) have identified a second D_2 receptor that is identical to the receptor cloned by Bunzow et al. (1988), but that contains an additional 87 bp sequence encoding 29 amino acids in the putative third cytosolic loop. The function of these 2 receptor isoforms is presently unclear, but preliminary results from this laboratory (unpublished observations) suggest that they have the same distribution in the rat CNS. The cRNA probes used in the present study, however, cannot differentiate between these receptor forms. Given that the insertion is within the third cytosolic loop, some investigators have speculated that it may be involved in coupling to G-proteins (Dal Toso et al., 1989; Giros et al., 1989; Monsma et al., 1989).

Many of the anatomical speculations raised in this manuscript are difficult to address at present. The development of antibodies and immunohistochemical D_2 receptor studies, in conjunction with tract-tracing, will provide a better understanding of the anatomical distribution of D_2 receptors and compliment these receptor autoradiography and *in situ* hybridization results. While such studies are important in understanding the anatomy of the D_2 receptor, it is clear even from the present results that the point of receptor insertion varies markedly among the neurons expressing D_2 receptors. In the case of cells in the substantia nigra, for example, the D_2 receptor is transported to the somatic and dendritic membranes, allowing visualization of a colocalization with the D_2 receptor mRNA. Neurons in other brain regions, such as the zona incerta, express D_2 receptors that are transported, most likely, to terminal fields, resulting in a discrepancy in the localization of D_2 receptor mRNA and binding. While several studies (e.g., Van Der Kooy et al., 1986; Aiso et al., 1987) have demonstrated that receptors are transported via fast axonal flow, the cellular mechanism controlling receptor transport and subsequent membrane insertion is largely unknown (Cullen et al., 1988; Gamou and Shimizu, 1988).

In conclusion, the present study is an initial anatomical examination of the distributions of D_2 receptor binding sites and mRNA. It combines receptor autoradiographic and *in situ* hybridization techniques to demonstrate brain regions of good correspondence between the binding site and mRNA and other areas of poor correspondence and possible receptor transport. In addition, it provides a framework for future coregulation studies and a means of asking more intelligent questions concerning the distribution of dopamine receptors and their possible function in the nervous system. If D_2 receptors prove to be similar to the other G-protein coupled receptors that have been cloned (e.g., muscarinic, α- and β-adrenergic), one might expect that there may be several receptor subtypes that encode for pharmacologically similar receptor binding sites, making future studies relating D_2 receptor mRNA(s) and D_2 binding sites even more challenging.

References

Aiso M, Potter WZ, Saavedra JM (1987) Axonal transport of dopamine D_1 receptors in the rat brain. Brain Res 426:392–396.

Attie MF, Brown EM, Gardner DG, Spiegel AM, Aurbach GD (1980) Characterization of dopamine-responsive adenylate cyclase of bovine parathyroid cells and its relationship to parathyroid hormone secretion. Endocrinology 107:1776–1781.

Billard W, Ruperto V, Crosby G, Iorio LC, Barnett A (1984) Characterization of the binding of [^{3}H] SCH23390, a selective D_1 receptor antagonist ligand, in rat striatum. Life Sci 35:1885–1893.

Bouthenet M-L, Martres MP, Sales N, Schwartz JC (1987) A detailed mapping of dopamine D_2 receptors in rat central nervous system by autoradiography with [^{125}I]Iodosulpride. Neuroscience 20:117–155.

Boyson SJ, McGonigle P, Molinoff PB (1986) Quantitative autoradiographic localization of the D_1 and D_2 subtypes of dopamine receptors in rat brain. J Neurosci 6:3177–3188.

Brown F, Campbell W, Mitchell PJ, Randall K (1985) Dopamine autoreceptors and the effects of drugs on locomotion and dopamine synthesis. Br J Pharmacol 84:853–860.

Bunzow JR, Van Tol HHM, Grandy DK, Albert P, Salon J, Christie M, Machida CA, Neve KA, Civelli O (1988) Cloning and expression of a rat D_2 dopamine receptor cDNA. Nature 336:783–787.

Charuchinda C, Supavilai P, Karobath M, Palacios JM (1987) Dopamine D_2 receptors in the rat brain: autoradiographic visualization using a high affinity selective agonist ligand. J Neurosci 7:1352–1360.

Clark D, Galloway MP (1985) Effects of 3-PPP enantiomers, SKF38393, and 8-OHDPAT on synthesis in mesocortical dopamine neurons. Soc Neurosci Abstr 11:1208.

Creese I, Burt DR, Snyder SH (1977) Dopamine receptor binding enhancement accompanies lesion-induced behavioral supersensitivity. Science 197:596–598.

Cross AJ, Waddington JL (1981) Kainic acid lesions dissociate [^{3}H] spiperone and [^{3}H] cisflupenthixol binding sites in rat striatum. Eur J Pharmacol 71:327–332.

Cullen BR, Podlask FJ, Peffer NJ, Hosking JB, Greene WC (1988) Sequence requirements for ligand binding and cell surface expression of the Tac antigen, a human interleukin-2 receptor. J Biol Chem 263: 4900–4906.

Dal Toso R, Sommer B, Ewert M, Herb A, Pritchett DB, Bach A, Shivers BD, Seeburg PH (1989) The dopamine D_2 receptor: two molecular forms generated by alternative splicing. EMBO J 8:4025–4034.

Dawson TM, Gehlert DR, McCabe RT, Barnett A, Wamsley JK (1986) D_1 dopamine receptors in the rat brain: a quantitative autoradiographic analysis. J Neurosci 6:2352–2365.

DeSouza EB (1986) Serotonin and dopamine receptors in the rat pituitary gland: autoradiographic identification, characterization and localization. Endocrinology 119:1534–1542.

Dubois A, Savasta M, Curet O, Scatton B (1986) Autoradiographic distribution of the D_1 agonist [^{3}H] SKF38393, in the rat brain and spinal cord. Comparison with the distribution of D_2 dopamine receptors. Neuroscience 19:125–137.

Filloux F, Dawson TM, Wamsley JK (1988) Localization of nigrostriatal dopamine receptor subtypes and adenylate cyclase. Brain Res Bull 20:447–459.

Gamou S, Shimizu N (1988) Glycosylation of the epidermal growth factor receptor and its relationship to membrane transport and ligand binding. J Biochem 104:388–396.

Giros B, Sokoloff P, Martres M-P, Riou J-F, Emorine LJ, Schwartz J-D (1989) Alternative splicing directs the expression of two D_2 dopamine receptor isoforms. Nature 342:923–926.

Halasz N, Shepherd GM (1983) Neurochemistry of the vertebrate olfactory bulb. Neuroscience 10:579–619.

Iorio LC, Barnett A, Leitz FH, Houser VP, Korduba CA (1983) SCH23390, a potential benzazepine antipsychotic with unique inter-

actions on dopaminergic systems. J Pharmacol Exp Ther 226:462–468.

Joyce JN, Marshall JF (1987) Quantitative autoradiography of dopamine D_2 sites in rat caudate-putamen: localization to intrinsic neurons and not to neocortical afferents. Neuroscience 20:773–795.

Kohler C, Fahlberg K (1985) Specific *in vivo* binding of [^{3}H] spiperone to individual lobes of the pituitary gland of the rat. Evidence for labelling of dopamine receptors. J Neural Trans 63:39–52.

Kohler C, Hall H, Ogren S-O, Gawell L (1985) Specific *in vitro* and *in vivo* binding of [^{3}H] raclopride. Biochem Pharmacol 34:2251–2259.

Mansour A, Meador-Woodruff JH, Camp DM, Robinson TE, Bunzow J, Van Tol HHM, Civelli O, Akil H, Watson SJ (1990) The effects of nigrostriatal 6-hydroxydopamine lesions on dopamine D_2 receptor mRNA and opioid systems. In: The international narcotics research conference (INRC) 1989 (Quirion, Jhamadas, and Gianoulakis, eds), pp 227–230. New York: Alan R Liss.

Martres M-P, Sales N, Bouthenet ML, Schwartz JC (1985) Localisation and pharmacological characterisation of D_2 dopamine receptors in rat cerebral neocortex and cerebellum using [^{125}I] Iodosulpride. Eur J Pharmacol 118:211–219.

Meador-Woodruff JH, Mansour A, Bunzow JR, Van Tol HHM, Watson SJ, Civelli O (1989) Distribution of D_2 dopamine receptor mRNA in rat brain. Proc Natl Acad Sci USA 86:7625–7628.

Memo M, Missale C, Carruba MO, Spano PF (1986) D_2 dopamine receptors associated with inhibition of dopamine release from rat neostriatum are independent of cyclic AMP. Neurosci Lett 71:192–196.

Monsma FJ Jr, McVittle LD, Gerfen LR, Mahan LC, Sibley DR (1989) Multiple D_2 dopamine receptors produced by alternative RNA splicing. Nature 342:926–929.

Munson PJ, Rodbard D (1980) Ligand: a versatile computerized approach for characterization of ligand-binding systems. Anal Biochem 107:220–239.

Nagy JI, Lee T, Seeman P, Fibiger HC (1978) Direct evidence for presynaptic and postsynaptic dopamine receptors in brain. Nature 274:278–281.

Onali P, Olianas MC, Gessa GL (1985) Characterization of dopamine receptors mediating inhibition of adenylate cyclase activity in rat striatum. Mol Pharmacol 28:138–145.

Paxinos G, Watson C (1986) The rat brain in stereotoxic coordinates. New York: Academic Press.

Pazos A, Stoeckel ME, Hindelang C, Palacios JM (1985) Autoradiographic studies on dopamine D_2 receptors in rat pituitary: influence of hormonal states. Neurosci Lett 59:1–7.

Porceddu ML, Giorgi O, Ongini E, Mele S, Biggio G (1986) [^{3}H] SCH23390 binding sites in the rat substantia nigra: evidence for a presynaptic localization and innervation by dopamine. Life Sci 39: 321–328.

Reisine TD, Nagy JI, Beaumont K, Fibiger HC, Yamamura HI (1979) The localization of receptor binding sites in the substantia nigra and striatum of the rat. Brain Res 177:241–252.

Richfield EK, Young AB, Penney JB (1987) Comparative distribution of dopamine D_1 and D_2 receptors in the basal ganglia of turtles, pigeons, rats, cats and monkeys. J Comp Neurol 262:446–463.

Schwarcz R, Creese I, Coyle JT, Snyder SH (1978) Dopamine receptors localised on cerebral cortical afferents to rat corpus striatum. Nature 271:766–768.

Stoof JC, Kebabian JW (1984) Two dopamine receptors: biochemistry, physiology and pharmacology. Life Sci 35:2281–2296.

Stoof JC, De Boer T, Sminia P, Mulder AH (1982) Stimulation of D_2 dopamine receptors in rat neostriatum inhibits the release of acetylcholine and dopamine but does not affect the release of gamma-aminobutyric acid, glutamate or serotonin. Eur J Pharmacol 84:211–214.

Trugman JM, Wooten GF (1987) Selective D_1 and D_2 agonists differentially alter basal ganglia glucose utilization in rats with unilateral 6-hydroxydopamine substantia nigra lesions. J Neurosci 7:2927–2935.

Van Der Kooy D, Weinreich P, Nagy JI (1986) Dopamine and opiate receptors: localization in the striatum and evidence for their axoplasmic transport in the nigrostriatal and striatonigral pathways. Neuroscience 19:139–146.

Wamsley JK, Gehlert DR, Filloux FM, Dawson TM (1989) Comparison of the distribution of D_1 and D_2 dopamine receptors in the rat brain. J Comp Neuroanat 2:119–137.

White FJ, Wang RJ (1983) Differential effects of classical and atypical antipsychotic drugs on A9 and A10 dopamine neurons. Science 221: 1054–1057.